

## RAY THEORY FOR HIGH-PÉCLET-NUMBER CONVECTION-DIFFUSION\*

S. J. CHAPMAN<sup>†</sup>, J. M. H. LAWRY<sup>†</sup>, AND J. R. OCKENDON<sup>†</sup>

**Abstract.** Asymptotic methods based on those of geometrical optics are applied to some steady convection-diffusion streamed flows at a high Péclet number. Even with the assumption of inviscid, irrotational flow past a body with uniform ambient conditions, the rays from which the solution is constructed can only be found after local analyses have been carried out near the stagnation points. In simple cases, the temperature away from the body is the sum of contributions from each stagnation point.

**Key words.** heat and mass transfer, asymptotic expansions, parabolic equations

**AMS subject classifications.** 80A20, 35K20, 41A60

**PII.** S0036139998344088

**1. Introduction.** The problem of determining the temperature  $T$  (or the contaminant concentration) in a prescribed steady fluid flow  $\mathbf{u}$  involves the solution of the nondimensional equation

$$(1.1) \quad \mathbf{u} \cdot \nabla T = \varepsilon \nabla^2 T,$$

where, in many practical cases such as high-Prandtl-number flows, the inverse Péclet number  $\varepsilon$  is small. In this paper we will make some remarks about the structure of the solution in cases when the flow streams two-dimensionally, with prescribed temperature  $T_\infty$  (not necessarily constant) at large distances from a finite impenetrable obstacle  $\Gamma$  at which certain boundary conditions are prescribed.

Problems of this type have been considered by authors too numerous to cite here, but the papers [7, 8] are particularly relevant to our work: there  $\mathbf{u}$  is taken to be of constant magnitude and direction which means that the flow can penetrate the obstacle, but the resulting asymptotic analysis reveals an interesting boundary-layer structure near the obstacle and a downstream wake or “shadow” that is reminiscent of the patterns of light intensity encountered in geometrical optics. Indeed the methodology we will adopt for solving (1.1) will be analogous to ray theory, and the principal motivation for the methodology applies equally to geometrical optics: the few explicit solutions that are available often take the form of infinite series that converge only slowly when the solution varies on scales much smaller than those dictated by the geometry. These variations take the form of high-frequency oscillations in wave propagation problems and boundary-layer behavior in diffusion problems, and the numerical algorithms are often costly.

The main part of this paper will describe the detailed asymptotic solution of a prototypical two-dimensional problem in which  $\mathbf{u}$  takes a particularly simple form, but before we embark on this we make some general remarks about the features we expect the solution to exhibit.

---

\*Received by the editors September 1, 1998; accepted for publication (in revised form) March 25, 1999; published electronically December 3, 1999. The research of the first author was supported by a Royal Society University Research Fellowship.

<http://www.siam.org/journals/siap/60-1/34408.html>

<sup>†</sup>OClAM, Mathematical Institute, 24–29 St Giles, Oxford OX1 3LB, UK (chapman@maths.ox.ac.uk, lawry@maths.ox.ac.uk, ejam@maths.ox.ac.uk).

We assume from the outset that the boundary conditions at the obstacle prohibit a solution in the form of a regular perturbation expansion in which the leading-order temperature field satisfies

$$\mathbf{u} \cdot \nabla T_0 = 0 \quad \text{with } T_0 \sim T_\infty \text{ as } |x| \rightarrow \infty$$

up to and including the boundary of the obstacle. For such problems we expect the conventional structure in which there is an “outer” solution away from the obstacle in which  $T \simeq T_0$  and an “inner” thermal boundary layer that is increasingly thin as  $\varepsilon \rightarrow 0$ . For example, if the temperature or heat flux is prescribed at the obstacle, we expect the boundary-layer thickness to be  $\mathcal{O}(\varepsilon^{1/2})$  or  $\mathcal{O}(\varepsilon^{1/3})$  depending on whether the fluid is inviscid or viscous, respectively. However, these orders of magnitude may change if a heat transfer boundary condition is imposed and also in the vicinity of stagnation and separation points on the obstacle. We will return to these complications later.

In many situations, higher-order corrections to this asymptotic scenario can be found quite simply. Away from the boundary,  $T$  can be expanded as  $T \sim T_0 + \varepsilon T_1 + \dots$ , where  $\mathbf{u} \cdot \nabla T_1 = \nabla^2 T_0$  etc., to obtain successively improved algebraically small improvements for small  $\varepsilon$ . These improvements account for local diffusion superimposed on dominant convection. This calculation would go hand in hand with improved boundary-layer corrections that match with the outer corrections at each stage of the iteration. However, one situation in which this procedure yields no information is when  $T_\infty$  is constant, so that the fluid is nearly isothermal away from the thermal boundary layers. In such a case the correction to  $T_\infty$  is exponentially small in  $\varepsilon$  away from these layers.<sup>1</sup> Furthermore, because these exponentially small corrections originate at the boundary, they can only be found from a global calculation rather than the local iteration described above, which just requires integration along the streamlines. The question immediately arises as to which points in the boundary have the greatest effect on the temperature correction at any point in the flow, and this is one of the crucial aspects of the following analysis.

In section 2 we give a brief description of the application of ray theory to (1.1), and then in section 3 we describe in detail what happens when  $T_\infty = 0$  and  $\mathbf{u}$  is inviscid and irrotational and the boundary is isothermal: this two-dimensional configuration is one that is relatively simple to explain yet interesting enough to be a paradigm for the more general situations to which we refer in the conclusion.

**2. The ray method for convection-diffusion in two dimensions.** We consider (1.1) with  $T \rightarrow 0$  as  $x^2 + y^2 \rightarrow \infty$  and  $T = 1$  on a smooth closed impenetrable body  $\Gamma$ . Because an expansion in powers of  $\varepsilon$  would yield no information, we consider the effect of applying the WKB ansatz

$$(2.1) \quad T = \varepsilon^\sigma \exp(\Phi/\varepsilon) (A_0 + \varepsilon A_1 + \dots),$$

with the assumption that  $\varepsilon \ll 1$ . The constant  $\sigma$  will be chosen to make the leading-order equation nontrivial. This technique allows the rapid exponential decay in  $T$  characteristic of small diffusivity to be captured in the slowly varying quantities  $\Phi$  and  $A_j$ , with immediate computational and theoretical advantages. This approach is widely used in problems in wave propagation in the frequency domain [6, 1, 2], where  $-i\Phi$  corresponds to the phase of a wave and the  $A_j$  are the amplitude coefficients:

---

<sup>1</sup>Indeed such exponentially small corrections occur for more general  $T_\infty$  and, if  $\varepsilon$  is not too small, then this can make an observable contribution to the temperature field, as can happen in high-frequency wave propagation.

there the ansatz (2.1) is applied to the Helmholtz equation or a variant and the limit  $\varepsilon \rightarrow 0$  corresponds to the high-frequency limit. The ansatz (2.1) may also be applied to other equations [4] including the convection-diffusion equation [10, 9], and the following procedure is taken from those papers.

Applying (2.1) to (1.1), we obtain at leading order

$$(2.2) \quad (\nabla\Phi)^2 - \mathbf{u} \cdot \nabla\Phi = 0,$$

which is the equivalent to the eikonal equation of geometrical optics. Its characteristics are solutions of

$$(2.3) \quad \dot{\mathbf{x}} = \mathbf{u} - 2\mathbf{p},$$

$$(2.4) \quad \dot{\mathbf{p}} = -(\mathbf{p} \cdot \nabla) \mathbf{u} + (\nabla \wedge \mathbf{u}) \wedge \mathbf{p},$$

$$(2.5) \quad \dot{\Phi} = -\mathbf{p} \cdot \mathbf{u} = -|\mathbf{p}|^2$$

with  $\mathbf{p} = \nabla\Phi$  and where a dot denotes differentiation along the characteristic. We see from (2.5) that  $\Phi$  decreases along a characteristic, corresponding to exponential decay of the quantity  $T$ .

Equating higher orders in  $\varepsilon$  give the transport equations

$$(2.6) \quad \mathbf{u} \cdot \nabla A_j = 2\nabla\Phi \cdot \nabla A_j + A_j \nabla^2 \Phi + \nabla^2 A_{j-1} \quad (j = 0, 1, 2, \dots),$$

where  $A_{-1} \equiv 0$ . These may be rewritten as ordinary differential equations in the parameter along the characteristics of (2.2), whence

$$(2.7) \quad \dot{A}_j - A_j \nabla^2 \Phi = \nabla^2 A_{j-1}.$$

If we use  $t$  to parametrize a characteristic (so that the dots in (2.3) and (2.7) represent  $\partial/\partial t$ ) and label the characteristics (perhaps by parametrization of the initial data) by  $s$ , then we may calculate the Jacobian

$$(2.8) \quad J = \frac{\partial(x, y)}{\partial(s, t)}$$

of the mapping from characteristic coordinates to space coordinates. This satisfies the transport equation

$$(2.9) \quad \dot{J} = J (\nabla \cdot \mathbf{u} - 2\nabla^2 \Phi),$$

which in combination with (2.7) gives

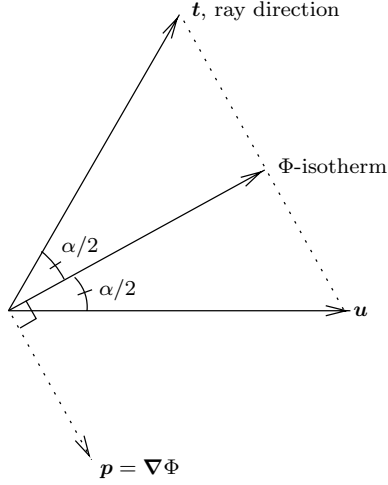
$$(2.10) \quad \frac{\partial}{\partial t} (A_j^2 J) = A_j^2 J \nabla \cdot \mathbf{u} + 2A_j J \nabla^2 A_{j-1}.$$

Hence if the flow is incompressible, then the quantity  $A_0^2 J$  is conserved. (This is also analogous to the equivalent conserved quantity in geometrical optics, where it may be interpreted as conservation of energy in a pencil of rays.)

We see from (2.2) that curves on which  $\Phi$  is constant have the vector  $\mathbf{u} - \mathbf{p}$  as tangent. Since to leading order these coincide with curves of constant  $T$ , we will call them isotherms. The tangent vector field to these curves bisects the angle formed by the ray (with direction  $\mathbf{t} = \mathbf{u} - 2\mathbf{p}$ ) and the flow  $\mathbf{u}$  at each point (see Figure 2.1).

We note that if we write  $\mathbf{t} = \dot{\mathbf{x}} = \mathbf{u} - 2\mathbf{p}$  for the direction of a characteristic, then

$$(2.11) \quad \mathbf{t}^2 = \mathbf{u}^2$$

FIG. 2.1. The orientation of the three vector fields  $\mathbf{u}$ ,  $\mathbf{p}$ , and  $\mathbf{t}$ .

and now the ray equations become

$$(2.12) \quad \dot{\mathbf{t}} = -\mathbf{t} \wedge (\nabla \wedge \mathbf{u}) + \nabla \left( \frac{1}{2} \mathbf{u}^2 \right), \quad \dot{\Phi} = -|\mathbf{u}|^2 \sin^2(\alpha/2),$$

where  $\alpha$  is the angle between the ray direction  $\mathbf{t}$  and the flow  $\mathbf{u}$ . Hence the quantity  $T$  decays exponentially along a ray at a rate that depends on the angle between the ray and flow.

In the next section we will need not only this basic version of ray theory, but also the methodology of the geometrical theory of diffraction (GTD) [6]. In simple terms, GTD states that whenever the ansatz (2.1) breaks down (e.g., at caustics), or whenever there is a singularity in the boundary data, an “inner” region needs to be introduced whose solution is matched with the outer ray solution. These regions may or may not include the thermal boundary layers referred to in the introduction, but in any case they are analogous to those regions in optics where diffraction occurs. In these regions, “inner” diffraction problems must be solved to provide initial data for the ray equations (2.3)–(2.5).

**3. Inviscid irrotational flow.** Throughout this section, we assume that  $\mathbf{u}$  is such that  $\nabla \wedge \mathbf{u} = \mathbf{0}$  and  $\mathbf{u} \cdot \mathbf{n} = 0$  on the boundary of  $\Gamma$ , where  $\mathbf{n}$  is the normal, and that there is no circulation around  $\Gamma$ . This immediately enables us to make a number of helpful observations.

First, the quantity  $|\mathbf{u}|$  corresponds to the refractive index of the medium; if this quantity is constant, then the rays are straight lines. Second, by Bernoulli’s theorem, the quantity  $p/\rho + \frac{1}{2} \mathbf{u}^2$  is constant throughout the flow (where  $p$  is the pressure of the fluid and  $\rho$  is the density), and hence the characteristics bend toward regions of low pressure, just as the rays of geometrical optics bend toward regions of high refractive index. Furthermore, we can construct a velocity potential  $\phi$  and stream function  $\psi$  such that  $\mathbf{u} = \nabla \phi = \nabla \wedge \psi \mathbf{k}$ . In the  $(\phi, \psi)$  coordinate system, the problem reduces (upon redefining  $x = \phi$ ,  $y = \psi$ ) to

$$(3.1) \quad \frac{\partial T}{\partial x} = \varepsilon \left( \frac{\partial^2 T}{\partial x^2} + \frac{\partial^2 T}{\partial y^2} \right);$$

in other words, we may conformally map the inviscid flow past a finite body onto uniform flow past a finite flat plate parallel to the flow  $\mathbf{u} = (1, 0)$ , and the equation for  $T$  is also preserved by this mapping (see Figure 3.1). The boundary condition on the plate is  $T = 1$ . The front and rear ends of the plate correspond to the stagnation points in the flow around the original body. Without loss of generality, we choose the ends of the plate to be at  $(0, 0)$  and  $(1, 0)$ . By (2.12), it follows that in the stream-function/velocity-potential coordinates, the characteristics (to which we will henceforth refer as rays) are straight lines.

Of course, the mapping from (1.1) to (3.1) holds for all Péclet numbers, and an exact solution may be found by separating the equation in elliptic coordinates and writing the solution as an infinite sum of products of Mathieu and modified Mathieu functions [3]. We expect the asymptotic expansion of this solution for a large Péclet number to agree with the asymptotic solution we will obtain by direct asymptotic methods applied to (3.1). A start has been made on such comparisons in [3], where the surface heat flux (which is algebraic in  $\varepsilon$ ) computed from the boundary layer solutions have been compared with those resulting from the explicit eigenfunction expansion of the solution. The agreement is good for  $\varepsilon < 1/2$ , but it is much harder to make comparisons away from the boundary because of the slow convergence of these series in the region where  $T$  is exponentially small. It would be interesting to know if procedures such as the Watson transform [5], which are useful in converting eigenfunction expansion solutions of Helmholtz equation into integrals suitable for asymptotic computation, can be applied to the series in [3], but we know of no results in that direction.

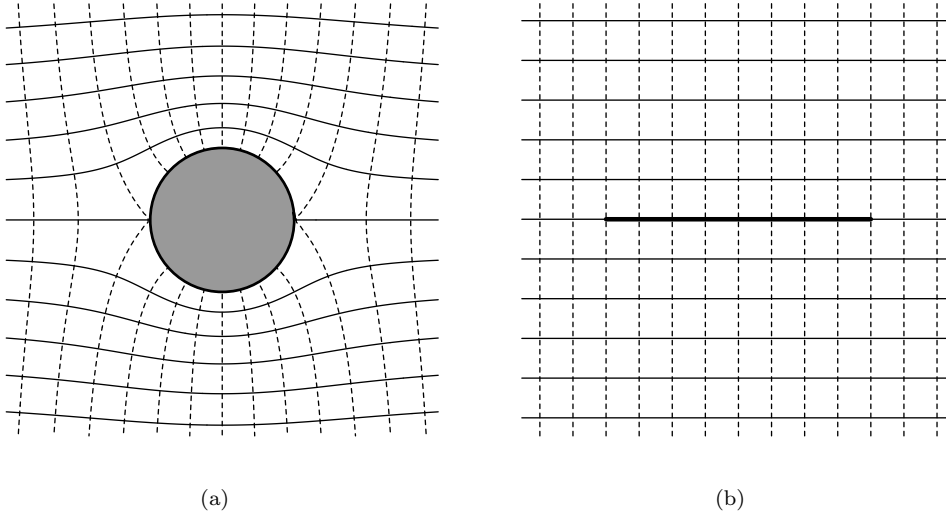


FIG. 3.1. *Inviscid irrotational flow past (a) a circular cylinder and (b) a flat plate. Curves of constant stream-function (solid) and constant velocity potential (dashed) are shown.*

For the paradigm problem (3.1) with  $T = 1$  at the plate and  $T_\infty = 0$ , we now address the key questions of where the rays originate and what initial data they must satisfy. First we note that if we attempt to give  $\Phi_0 = 0$  as initial data on  $x_0 = s$ ,  $y_0 = 0$  ( $0 < s < 1$ ), then we find that  $p_0 = 0$ ,  $q_0 = 0$  so that none of the rays leaves the

plate. However, following the methodology of GTD we expect rays to be generated (“diffracted”) at points where the boundary is not smooth. Thus we will begin by considering the inner “diffraction” problem in the vicinity of the leading edge of the plate, whose far field should provide us with initial data for the ray equations.

**3.1. Leading edge.** Near the leading edge of the plate, a rescaling of the coordinates

$$(3.2) \quad x = \varepsilon \tilde{x}, \quad y = \varepsilon \tilde{y}$$

results in (3.1) taking the form

$$(3.3) \quad \frac{\partial T}{\partial \tilde{x}} = \frac{\partial^2 T}{\partial \tilde{x}^2} + \frac{\partial^2 T}{\partial \tilde{y}^2},$$

with boundary and matching conditions

$$(3.4) \quad T = 1 \quad (\tilde{y} = 0, \tilde{x} > 0),$$

$$(3.5) \quad \frac{\partial T}{\partial \tilde{y}} = 0 \quad (\tilde{y} = 0, \tilde{x} < 0),$$

$$(3.6) \quad T \rightarrow 0 \quad \text{at infinity.}$$

Condition (3.5) results from the symmetry under reflection in the  $y$ -axis. The equation separates in parabolic coordinates  $\tilde{\xi}, \tilde{\eta}$  where  $\tilde{x} = \tilde{\xi}^2 - \tilde{\eta}^2$ ,  $\tilde{y} = 2\tilde{\xi}\tilde{\eta}$ , so that

$$(3.7) \quad \frac{\partial^2 T}{\partial \tilde{\xi}^2} + \frac{\partial^2 T}{\partial \tilde{\eta}^2} = 2 \left( \tilde{\xi} \frac{\partial T}{\partial \tilde{\xi}} - \tilde{\eta} \frac{\partial T}{\partial \tilde{\eta}} \right)$$

and the solution is

$$(3.8) \quad T = \operatorname{erfc} \tilde{\eta};$$

the isotherms are shown in Figure 3.2.

In the limit of large  $\tilde{\eta}$ , we have

$$(3.9) \quad T \sim \frac{1}{\tilde{\eta}\sqrt{\pi}} \exp(-\tilde{\eta}^2) = \frac{\csc(\theta_1/2)}{\sqrt{\pi r_1}} \exp\left[\frac{\tilde{x} - \tilde{r}_1}{2}\right],$$

where  $r_1, \theta_1$  are polar coordinates corresponding to  $x, y$ , and  $r_1 = \varepsilon \tilde{r}_1$ . This means that, in (2.1),  $\sigma = 1/2$  and the matching condition that the outer ray solution must satisfy near the leading edge is

$$(3.10) \quad \Phi \sim \frac{1}{2}(x - r_1), \quad A_0 \sim \frac{\csc(\theta_1/2)}{\sqrt{\pi r_1}}.$$

Higher-order amplitude coefficients  $A_j$  are determined by further terms in the asymptotic expansion of  $\operatorname{erfc}$ .

The implication for the outer ray solution is that  $\mathbf{t} = (x/r_1, y/r_1)$  and consequently a family of rays emanates radially from the leading edge of the plate, as shown in Figure 3.3. The amplitude coefficients are singular at the leading edge of the plate, but the leading-order amplitude  $A_0$  is of the form  $f(\theta_1)/\sqrt{r_1}$  where the directivity function  $f(\theta_1)$  has been found and is analogous to a diffraction coefficient in GTD. The behavior of  $A_0$  as  $r_1^{-1/2}$  follows from the shape of the rays and (2.10). We

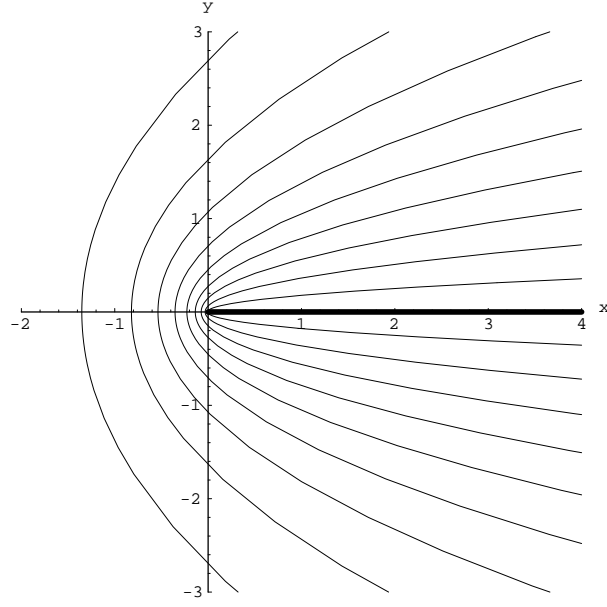


FIG. 3.2. Isotherms in the inner region near the leading edge of the plate.

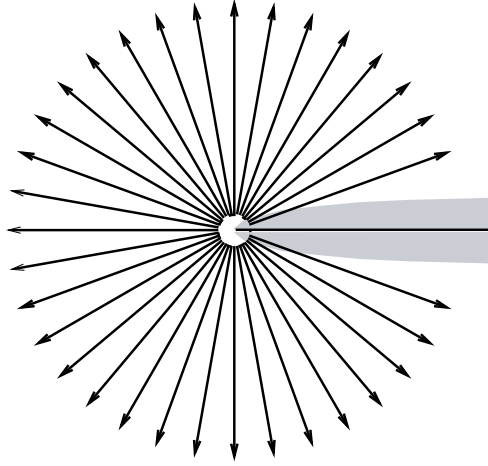


FIG. 3.3. Rays generated by the inner region at the leading edge of the plate (solid line). The shaded region denotes the area in which the ray approximation ceases to be valid.

note that the approximation (3.10) is valid for large  $\tilde{\eta}$ . Consequently the directivity is not uniform in  $\theta_1$  and in particular it is inaccurate for  $\theta_1$  near zero.

Note that the Green's function of (3.1) in  $\mathbb{R}^2$  is

$$(3.11) \quad T = \frac{1}{2\pi\varepsilon} \exp\left[\frac{x}{2\varepsilon}\right] K_0\left(\frac{r_1}{2\varepsilon}\right)$$

(for a point source at the origin) which also has an asymptotic expansion (2.1) in which

$$(3.12) \quad \Phi = \frac{1}{2}(x - r_1), \quad A_0 = \sqrt{\frac{\pi}{r_1}}, \quad \sigma = -\frac{1}{2}$$

(as  $\varepsilon \rightarrow 0$ ). As in GTD, the far field has  $A_0$  independent of polar angle. Hence the leading edge of the plate may be thought of as acting as a point source, but with directivity of amplitude  $\varepsilon \csc(\theta_1/2)/\sqrt{\pi}$ .

**3.2. Thermal boundary layer.** Since the ray approximation becomes singular at  $\theta = 0$  there is a further inner region close to the top of the plate where  $x = \mathcal{O}(1)$ ,  $y = \mathcal{O}(\varepsilon^{1/2})$ , with  $y > 0$ . With these scalings (3.1) takes the familiar thermal boundary-layer form

$$(3.13) \quad \frac{\partial T}{\partial x} = \frac{\partial^2 T}{\partial \hat{y}^2} + \varepsilon \frac{\partial^2 T}{\partial x^2},$$

where  $y = \sqrt{\varepsilon} \hat{y}$ . To leading order (3.13) has a similarity solution,

$$(3.14) \quad T = \operatorname{erfc} \left( \frac{\hat{y}}{2\sqrt{x}} \right),$$

which matches with (3.8) in the limit  $x \rightarrow 0$ ,  $\hat{y} \rightarrow 0$ . For future reference, we note that as  $\hat{y} \rightarrow 0$  and  $x = \mathcal{O}(1)$ ,

$$(3.15) \quad T \sim 1 - \frac{\hat{y}}{\sqrt{\pi x}} + \mathcal{O}(\hat{y}^3).$$

More important, in outer coordinates (3.14) is

$$(3.16) \quad \operatorname{erfc} \frac{y}{2\sqrt{\varepsilon x}} \sim \frac{2\sqrt{\varepsilon x}}{y\sqrt{\pi}} \exp \left[ -\frac{y^2}{4\varepsilon x} \right] \quad \text{as } \frac{y}{\sqrt{\varepsilon x}} \rightarrow \infty,$$

which matches into the near-field expansion of the ray solution (3.10). Thus no new rays emanate from this thermal boundary layer.

**3.3. Trailing edge.** The solution (3.14) fails to satisfy the boundary condition at the trailing edge of the plate. Hence there is a third inner region in the vicinity of the trailing edge, in which we use the scalings  $x = 1 + \varepsilon \bar{x}$ ,  $y = \varepsilon \bar{y}$  to obtain the equation

$$(3.17) \quad \frac{\partial T}{\partial \bar{x}} = \frac{\partial^2 T}{\partial \bar{x}^2} + \frac{\partial^2 T}{\partial \bar{y}^2},$$

with boundary conditions

$$(3.18) \quad T = 1 \quad (\bar{y} = 0, \bar{x} < 0),$$

$$(3.19) \quad \frac{\partial T}{\partial \bar{y}} = 0 \quad (\bar{y} = 0, \bar{x} > 0),$$

$$(3.20) \quad T \rightarrow 0 \quad \text{at infinity},$$

and a matching condition with the solution in section 3.2. This may be solved most easily by observing that if we write  $T = 1 + \varepsilon^{\frac{1}{2}} T_1$ , then  $S = \partial T_1 / \partial \bar{y}$  satisfies the same equation (3.17) in this region as  $T$ , but with boundary conditions

$$(3.21) \quad \frac{\partial S}{\partial \bar{y}} = 0 \quad (\bar{y} = 0, \bar{x} < 0),$$

$$(3.22) \quad S = 0 \quad (\bar{y} = 0, \bar{x} > 0)$$

(where we have differentiated (3.18) along the boundary and applied (3.17) to obtain (3.21)). Matching with (3.15) as  $x \rightarrow -\infty$ , we see that we require

$$(3.23) \quad S \rightarrow -\frac{1}{\sqrt{\pi}} \quad \text{as } \bar{x} \rightarrow -\infty.$$

This problem may be separated and solved in parabolic coordinates  $(\bar{\xi}, \bar{\eta})$  (with  $\bar{x} = \bar{\xi}^2 - \bar{\eta}^2$ ,  $\bar{y} = 2\bar{\xi}\bar{\eta}$ ) as for the leading edge, resulting in

$$(3.24) \quad S = \frac{\partial T_1}{\partial \bar{y}} = -\frac{1}{\sqrt{\pi}} \operatorname{erf} \bar{\eta} + \frac{C\bar{\eta}}{\pi(\bar{\xi}^2 + \bar{\eta}^2)} \exp(-\bar{\eta}^2)$$

for arbitrary constant  $C$ . Integrating, we find

$$(3.25) \quad T_1 = -\frac{\bar{y}}{\sqrt{\pi}} \operatorname{erf} \bar{\eta} - \frac{2}{\pi} \bar{\xi} \exp(-\bar{\eta}^2) + \frac{C+1}{\sqrt{\pi}} \exp(\bar{x}) \operatorname{erf} \bar{\xi} + A(\bar{x})$$

where  $A$  is arbitrary. However  $A(\bar{x})$  vanishes for  $\bar{x} \leq 0$  from (3.18) and  $T_1$  is an analytic function of  $(\bar{x}, \bar{y})$ , so  $A \equiv 0$ , and we must choose  $C = -1$  to satisfy the requirement that  $T_1$  grows subexponentially as  $\bar{x} \rightarrow +\infty$ . Consequently we have the solution

$$(3.26) \quad T = 1 - \left(\frac{\varepsilon}{\pi}\right)^{1/2} \left( \bar{y} \operatorname{erf} \bar{\eta} + \frac{2\bar{\xi}}{\sqrt{\pi}} \exp(-\bar{\eta}^2) \right).$$

The outer limit of this, letting  $\bar{x}, \bar{y} = \mathcal{O}(\varepsilon^{-1})$ , is

$$(3.27) \quad T = 1 - \frac{\varepsilon^{-1/2}}{\sqrt{\pi}} y - \frac{\varepsilon}{\pi} \frac{\xi}{\eta^2} \exp(-\eta^2/\varepsilon) (1 + \mathcal{O}(\varepsilon)).$$

Here  $y$  is the original outer Cartesian coordinate and  $\xi$  and  $\eta$  are now parabolic coordinates on the outer scale defined by  $x - 1 = \xi^2 - \eta^2$ ,  $y = 2\xi\eta$ .

Let us now try to unscramble the ray theory implications of (3.27). We can identify the first term in (3.27) with that in (3.15). Indeed this identification allows us to think of a ray on which  $\Phi = 0$  that propagates downstream from the leading edge.

The presence of the second term in (3.27) is more troublesome and the fact that it is of  $\mathcal{O}(\varepsilon^{-1/2})$  necessitates the introduction of an intermediate matching region  $y = \mathcal{O}(\sqrt{\varepsilon})$ ,  $x - 1 = \mathcal{O}(\sqrt{\varepsilon})$ , in which (3.26) has the form

$$(3.28) \quad T \sim 1 - \frac{\hat{y}}{\sqrt{\pi}} - \frac{\varepsilon^{3/4}}{\pi} \frac{\hat{y}}{2\hat{\eta}^3} \exp(-\varepsilon^{-1/2}\hat{\eta}^2) \left(1 + \mathcal{O}(\varepsilon^{1/2})\right),$$

where  $\hat{\eta} = \varepsilon^{-1/4}\eta$ . In the intermediate region, with scaled coordinates  $x - 1 = \varepsilon^{1/2}\hat{x}$ ,  $y = \varepsilon^{1/2}\hat{y}$ , the scaled field equation is

$$(3.29) \quad \frac{\partial T}{\partial \hat{x}} = \varepsilon^{1/2} \left( \frac{\partial^2 T}{\partial \hat{x}^2} + \frac{\partial^2 T}{\partial \hat{y}^2} \right)$$

and so, in an expansion  $T \sim T_0 + \varepsilon^{1/2}T_1 + \dots$ , the leading-order solution,  $T_0$ , is independent of  $\hat{x}$ . Now (3.14) implies the matching condition  $T \sim \operatorname{erfc}(\hat{y}/2)$  as  $\hat{x} \rightarrow -\infty$ , and hence

$$T_0 \sim \operatorname{erfc}\left(\frac{\hat{y}}{2}\right).$$

Thankfully the third term on the right-hand side of (3.28) automatically satisfies (3.29). Hence the solution in the intermediate region  $\hat{y} = \mathcal{O}(1)$ ,  $\hat{x} = \mathcal{O}(1)$  is

$$(3.30) \quad T = \operatorname{erfc}\left(\frac{\hat{y}}{2}\right) + \mathcal{O}(\varepsilon^{1/2}) - \frac{\varepsilon^{3/4}}{\pi} \frac{\hat{y}}{2\hat{\eta}^3} \exp(-\varepsilon^{-1/2}\hat{\eta}^2) \left(1 + \mathcal{O}(\varepsilon^{1/2})\right).$$

Now if we take the outer limit we find

$$(3.31) \quad T = 1 + \mathcal{O}(\varepsilon) - \frac{\varepsilon}{\pi} \frac{\xi}{\eta^2} \exp(-\eta^2/\varepsilon) (1 + \mathcal{O}(\varepsilon)),$$

and we have succeeded in identifying where and how to write the local solution near the trailing edge in a form that can be used to match with the outer ray solution. Equations (3.30) and (3.31) look rather unusual in that we have neglected terms of algebraic order while including exponentially small ones, but the exponentially smaller terms correspond to the ray from the trailing edge.

When we proceed to construct a ray solution from the outer limit of (3.30), we find that the first term of (3.30) tends precisely to the expression for the ray from the leading edge, (3.9). However the last term corresponding to the ray from the trailing edge is unchanged from (3.27) and may be written as

$$(3.32) \quad \Phi = \frac{1}{2}(x - 1 - r_2), \quad A_0 = -\frac{\cot \frac{\theta_2}{2} \csc \frac{\theta_2}{2}}{\pi \sqrt{r_2}}, \quad \sigma = 1,$$

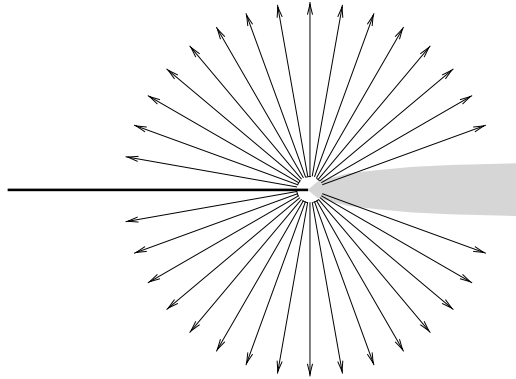


FIG. 3.4. Rays generated by the inner region at the trailing edge of the plate (solid line). The shaded region denotes the area in which the ray approximation ceases to be valid.

where  $r_2$ ,  $\theta_2$  are polar coordinates centered on the trailing edge  $x = 1$ ,  $y = 0$ . This corresponds to a fan of rays emanating from the trailing edge, as shown in Figure 3.4. Its leading-order amplitude coefficient  $A_0$  is negative, and hence its effect on the solution is subtractive, reflecting the fact that the temperature is lower than that for

a semi-infinite plate. The expression for  $A_0$  is singular along  $y = 0, x > 1$  and this will be smoothed with a further matching region in the next section. The coefficient of  $r_2^{-1/2}$  in the expression for  $A_0$  corresponds to a diffraction coefficient in GTD [6], just as (3.10) did for the leading edge. Other than the directivity function being different, the main difference between the two rays is  $\sigma$ : the “diffracted” contribution from the front is  $\mathcal{O}[\varepsilon^{1/2} \exp(-r_1 \sin^2(\theta_1/2)/\varepsilon)]$  at a distance  $R_1$  and angle  $\theta_1$  from the leading edge, while that from the rear is  $\mathcal{O}[\varepsilon \exp(-r_2 \sin^2(\theta_2/2)/\varepsilon)]$ . Note that the contribution from the leading edge is always exponentially dominant over the contribution from the trailing edge, except on the line  $y = 0, x > 1$  where the leading-edge ray is algebraically dominant over the trailing-edge ray by a factor proportional to  $\varepsilon^{1/2}$ . However, both ray approximations are nonuniform in this wake or “penumbral” region and consequently we must analyze it locally.

**3.4. Wake behind trailing edge.** In the region  $x - 1 = \mathcal{O}(1)$ ,  $y = \mathcal{O}(\sqrt{\varepsilon})$ , we may again use the scaled variable  $\hat{y} = y/\sqrt{\varepsilon}$ . Then  $T$  satisfies (3.13) to leading order. We write

$$X = \frac{x-1}{4}, \quad Y = \frac{\hat{y}}{2}.$$

Then in the region  $X > 0, Y > 0$  we are solving

$$\frac{\partial T}{\partial X} = \frac{\partial^2 T}{\partial Y^2}$$

to lowest order, with boundary conditions

$$T = \operatorname{erfc} Y \quad \text{on } X = 0, \quad \frac{\partial T}{\partial Y} = 0 \quad \text{on } Y = 0.$$

Then  $\tilde{T}$ , the cosine transform in  $Y$  of  $T$ , satisfies  $\tilde{T}_X = -p^2 \tilde{T}$  with boundary condition

$$\tilde{T} = \frac{1}{p} \operatorname{erfi}\left(\frac{p}{2}\right) \exp\left[-\frac{p^2}{4}\right] \quad \text{when } X = 0,$$

where  $\operatorname{erfi}(z) = -i \operatorname{erf}(iz)$  is the imaginary error function. Then the solution is

$$\tilde{T} = \frac{1}{p} \operatorname{erfi}\left(\frac{p}{2}\right) \exp\left[-p^2 \left(X + \frac{1}{4}\right)\right],$$

so inverting the transform gives

$$(3.33) \quad T = \frac{1}{2\sqrt{\pi X}} \int_0^\infty \exp\left[-\frac{s^2}{4X}\right] (\operatorname{erfc}(s+Y) + \operatorname{erfc}|Y-s|) \, ds$$

$$(3.34) \quad = \frac{1}{2\sqrt{\pi X}} \int_{-\infty}^\infty \exp\left[-\frac{(s+Y)^2}{4X}\right] \operatorname{erfc}|s| \, ds$$

which is

$$(3.35) \quad T = \frac{1}{\sqrt{\pi(x-1)}} \int_{-\infty}^\infty \exp\left[-\frac{(2\sqrt{\varepsilon}s+y)^2}{4\varepsilon(x-1)}\right] \operatorname{erfc}|s| \, ds.$$

in outer variables. Now if  $Y = 0$  then the integral in (3.34) may be evaluated exactly:

$$T = \frac{2}{\pi} \tan^{-1} \frac{1}{2\sqrt{X}} = \frac{2}{\pi} \tan^{-1} \sqrt{\frac{1}{x-1}}$$

which has asymptotic behavior

$$T \sim \frac{1}{\pi\sqrt{X}} + \mathcal{O}(X^{-3/2}), \quad X \rightarrow \infty.$$

For  $Y \rightarrow \infty$  ( $X = \mathcal{O}(1)$ ) we consider the asymptotics of (3.34). Writing the integral in this as

$$(3.36) \quad \int_0^\infty \operatorname{erfc} s \exp \left[ -\frac{(s+Y)^2}{4X} \right] ds + \left( \int_{-\infty}^\infty - \int_{-\infty}^0 \right) \operatorname{erfc} s \exp \left[ -\frac{(s-Y)^2}{4X} \right] ds,$$

we find we can integrate the first and third integrals in (3.36) by parts: the leading-order contributions cancel while the next orders double up to give

$$-\frac{16}{\sqrt{\pi}} \frac{X^2}{Y^2} \exp \left[ -\frac{Y^2}{4X} \right],$$

where the remaining integral is  $\mathcal{O}(Y^{-3})$ .

The second integral may be approximated using the method of steepest descent. Since we expect the main contribution to come from  $s = \mathcal{O}(Y)$ , we may replace  $\operatorname{erfc} s$  with its large-argument asymptotic expansion, giving a maximum contribution at  $s = s_0 = Y/(4X + 1)$ . Consequently the leading-order asymptotic approximation to the integral is

$$\frac{2\sqrt{X(4X+1)}}{Y} \exp \left[ -\frac{Y^2}{4X+1} \right].$$

Finally the asymptotic approximation to (3.33) is

$$(3.37) \quad T \sim \frac{\sqrt{4X+1}}{\sqrt{\pi}Y} \exp \left[ -\frac{Y^2}{4X+1} \right] - \frac{8X^{3/2}}{\pi Y^2} \exp \left[ -\frac{Y^2}{4X} \right]$$

which, in original variables, is

$$T \sim \frac{2}{\sqrt{\pi}} \varepsilon^{1/2} \frac{\sqrt{x}}{y} \exp \left[ -\frac{y^2}{4\varepsilon x} \right] - \frac{4\varepsilon (x-1)^{3/2}}{\pi y^2} \exp \left[ -\frac{y^2}{4\varepsilon(x-1)} \right]$$

and both terms are in ray form. Substituting with  $\tilde{\eta} \sim y/(2\sqrt{\varepsilon x})$ ,  $\bar{\eta} \sim y/(2\sqrt{\varepsilon(x-1)})$  matches each term with the outer limit of the leading and trailing edge inner solutions (3.9) and (3.27) exactly.

The genesis of the ray solution for the problem is summarized in Figure 3.5. The thermal boundary layer and wake can be thought of as rays tangent to the  $x$ -axis. All the other rays form the two distinct families that originate from inner regions of dimension  $\mathcal{O}(\varepsilon)$  near the leading and trailing edges, but those at the trailing edge have to penetrate an intermediate region of size  $\mathcal{O}(\varepsilon^{1/2})$  before they can be matched to the outer ray solution.

It is now a straightforward task to relate this scenario to irrotational flow past any body that can be mapped to the plate. For example, for a circular cylinder of unit radius, for which the conformal mapping to the plate is

$$(3.38) \quad \zeta(z) = z + \frac{1}{z}.$$

The ray paths are shown in Figure 3.6. As for the plate, there exists a thermal boundary layer on the cylinder and there is a thermal wake within  $\mathcal{O}(\varepsilon^{1/2})$  of the downstream stagnation streamline.

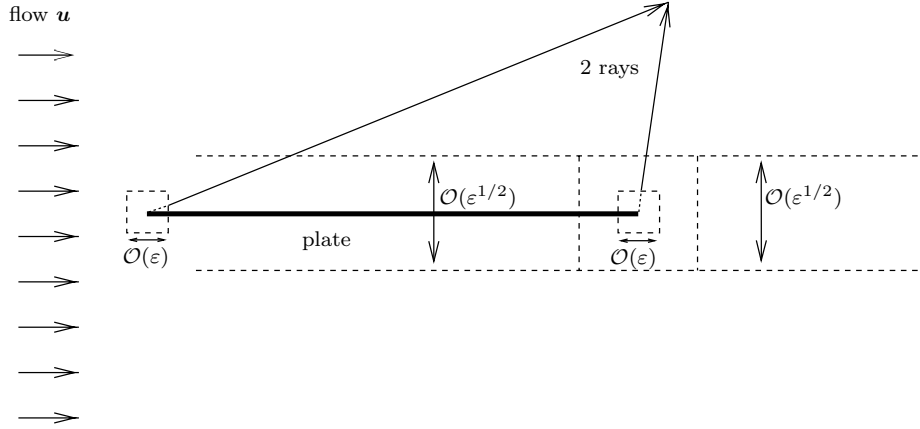


FIG. 3.5. The two rays present at every point in the domain of the problem.

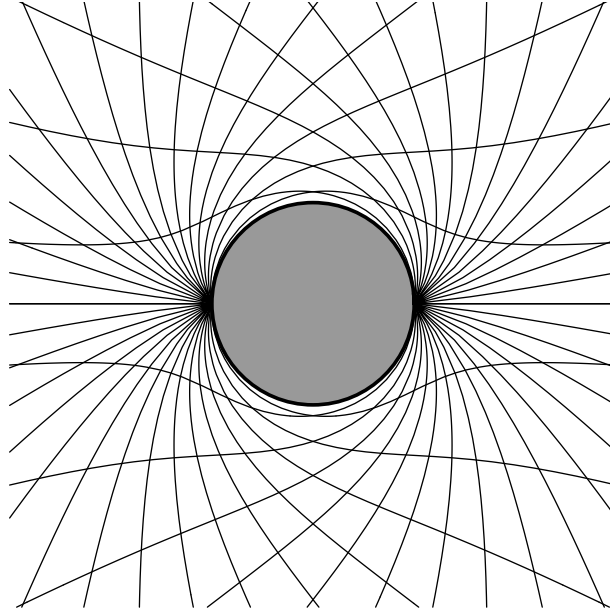


FIG. 3.6. Rays for the circular cylinder in uniform inviscid irrotational flow. Each point is the intersection of two rays, one from each stagnation point.

**4. Discussion and generalization.** The analysis of section 3 shows that rays of the outer solution for the temperature can only be generated at the upstream and downstream stagnation points on a smooth, isothermal body. In fact, we expect the same result to apply even if the body has corners on it at which the flow speed is zero or infinite, just as long as it can be mapped into a flat plate. We can even cater to separated Helmholtz flows, such as that past a flat plate at right angles to a stream as in Figure 4.1(a). We must now impose a boundary condition across the free surface of the flow, which we take to be a zero flux condition,

$$\frac{\partial T}{\partial n} = 0 \quad \text{on the free surface.}$$

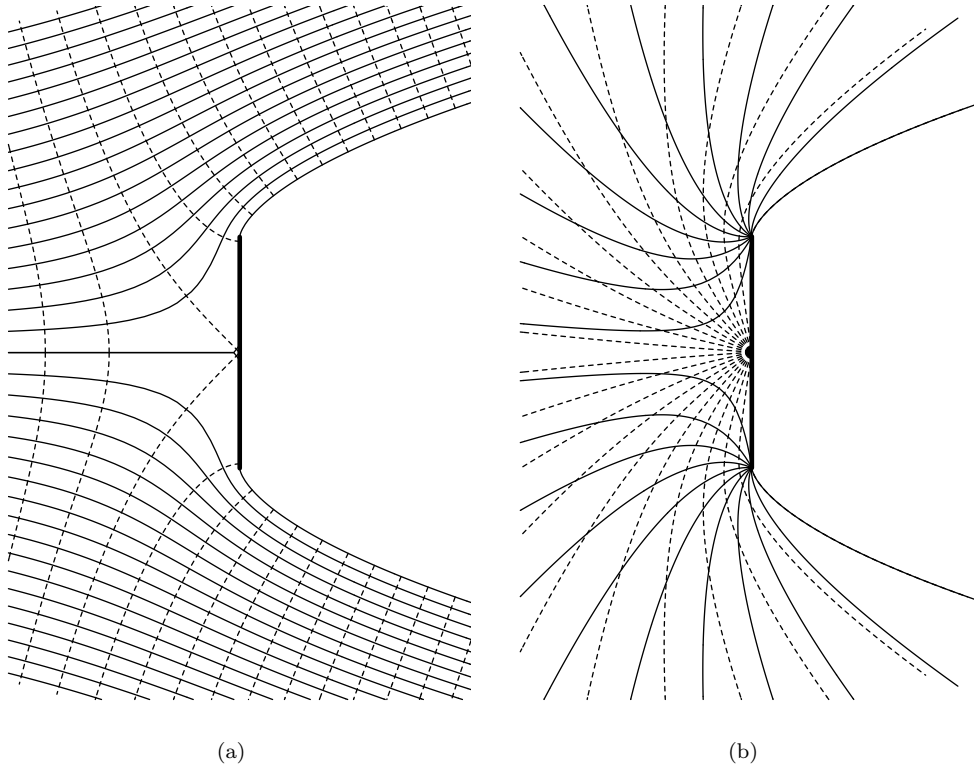


FIG. 4.1. (a) A separated flow (solid streamlines, dashed curves of constant velocity potential) past a flat plate at right angles to the flow. (b) Rays for this flow: one family from stagnation point (dashed) and one from each separation point (solid).

This means that the structure of the solution is unchanged from section 3 because we may conformally map the flow to that shown in Figure 3.1(b), but with a branch cut extending from the trailing edge of the plate parallel to the flow. The edges of the regions immediately above and below the branch cut correspond to the free surfaces extending from the upper and lower edges, respectively, of the plate. Since the solutions which we found in sections 3.3 and 3.4 already satisfy  $\partial T / \partial n = 0$  across the line  $y = 0$  for  $x > 1$ , they are also the corresponding inner solutions in the corresponding regions of the separated flow. Consequently the ray solution is also as constructed for the unseparated case. Each separation point generates a fan of rays whose trajectories are straight in stream-function/velocity-potential coordinates (but curved in space coordinates), as shown in Figure 4.1(b).

The introduction of a sufficiently small circulation around  $\Gamma$  poses no difficulties to our theory. Even though the flow field can no longer be mapped one-to-one to the uniform stream of Figure 3.1(b), the local behavior near the leading and trailing stagnation points on a smooth body will be as in Figure 3.6. However, if the circulation is so great that a region of closed streamlines appears, a very different scenario emerges. Now a regular expansion is possible inside the region of closed streamlines, which suggests that  $T$  is linear in  $\psi$  (the stream function) there, with a thermal boundary layer on the separating streamline and an inner region near the stagnation point. We

would expect rays again to originate from the stagnation point, but now rays traveling into the region of closed streamlines reflect from the body as in geometrical optics. Thus there are again two rays through each point: one directly from the stagnation point, and one which has first been reflected.

A more difficult generalization is to viscous flow. The thermal boundary layers will still not generate any extra rays, but the inner problems near the stagnation points will now be more difficult to solve.

Finally we remark that our method should apply to nonisothermal bodies. Of particular mathematical interest would be cases where either the body temperature or the heat flux was so rapidly varying that  $\log T$  changed by  $\mathcal{O}(\varepsilon^{-1})$  on the body, or when the heat transfer coefficient was  $\mathcal{O}(\varepsilon^{-1})$ . In either case we would have the possibility that rays from the body could penetrate the interior of the flow and completely change the scenario in Figures 3.5 and 3.6.

**Acknowledgments.** The authors would like to thank Professor J. B. Keller for helpful discussions concerning this paper.

#### REFERENCES

- [1] V. M. BABIĆ AND V. S. BULDYREV, *Short-Wavelength Diffraction Theory—Asymptotic Methods*, Springer Ser. Wave Phenomena 4, Springer-Verlag, Berlin, 1991.
- [2] S. J. CHAPMAN, J. M. H. LAWRY, J. R. OCKENDON, AND R. H. TEW, *On the theory of complex rays*, SIAM Rev. 41 (1999), pp. 417–509.
- [3] G. P. CHEREPANOV, *Two-dimensional convective heat/mass transfer for low Prandtl and any Peclet numbers*, SIAM J. Appl. Math., 58 (1998), pp. 942–960.
- [4] J. K. COHEN AND R. M. LEWIS, *A ray method for the asymptotic solution of the diffusion equation*, J. Inst. Math. Appl., 3 (1967), pp. 266–290.
- [5] D. S. JONES, *Acoustic and Electromagnetic Waves*, Clarendon Press, Oxford, 1986.
- [6] J. B. KELLER, *A geometrical theory of diffraction*, in *Calculus of Variations and Its Applications*, Proc. Sympos. Appl. Math. 8, McGraw-Hill, New York, Toronto, London, 1958, pp. 27–32.
- [7] C. KNESSL AND J. B. KELLER, *Advection-diffusion past a strip. I. Normal incidence*, J. Math. Phys., 38 (1997), pp. 267–282.
- [8] C. KNESSL AND J. B. KELLER, *Advection-diffusion past a strip. II. Oblique incidence*, J. Math. Phys., 38 (1997), pp. 902–925.
- [9] R. SMITH, *The early stages of contaminant dispersion in shear flows*, J. Fluid Mech., 111 (1981), pp. 107–122.
- [10] R. SMITH, *Effect of non-uniform currents and depth variations upon steady discharges in shallow water*, J. Fluid Mech., 110 (1981), pp. 373–380.